



Co-production of Monosaccharides and Hydrochar from Green Macroalgae *Ulva* (Chlorophyta) sp. with Subcritical Hydrolysis and Carbonization

Semion Greiserman^{1,2} · Michael Epstein¹ · Alexander Chemodanov¹ · Efraim Steinbruch^{1,2} · Meghanath Prabhu¹ · Lior Guttman³ · Gabriel Jinjikhshvily⁴ · Olga Shamis⁵ · Michael Gozin⁵ · Abraham Kribus² · Alexander Golberg¹ 

© Springer Science+Business Media, LLC, part of Springer Nature 2019

Abstract

Subcritical water hydrolysis and carbonization of the biomass are an emerging green technology for seaweed biomass processing. In this work, a novel approach for co-generation of two energy streams from seaweed biomass (fermentable sugars and solid hydrochar) with subcritical water from a green macroalgae *Ulva* sp. was developed. It was found that for the released of glucose, xylose, rhamnose, fructose, and galactose, the process temperature is the most significant parameter, followed by salinity, solid load, and treatment time. For the formation of fermentation inhibitor 5-hydroxymethylfurfural (5-HMF), temperature also was the most important parameter, followed by residence time, salinity, and solid load. The optimum parameters for maximal release of total sugars under minimum formation of 5-HMF were 170 °C (800 kPa abs.), 5% solid loading, 40 min residence time, and 100% salinity. The hydrochar yield was 19.4% and hydrochar high heating value was 20.2 ± 1.31 MJ kg⁻¹. These results provide new detailed information on the subcritical hydrolysis and carbonization of *Ulva* sp. biomass and show co-production of fermentable monosaccharides and hydrochar.

Keywords Macroalgae · *Ulva* sp. · Biorefinery · Subcritical hydrolysis · Biomass deconstruction · Hydrochar · Fermentable monosaccharides

Introduction

Marine macroalgae, which contain very little lignin and do not compete with food crops for arable land or potable water, can provide a sustainable alternative source of biomass for food, fuel, and chemical generation [1]. One of the pathways to use

macroalgae feedstocks is to feed them as media for fermenting microorganisms [2]. A key step in the macroalgae conversion to chemicals and biofuels is the deconstruction of complex carbohydrates to fermentable sugars [3]. To increase the fermentation yields, pretreatment methods, which lead to the release of extracellular compounds and break the seaweed complex polysaccharides, are used. Various types of pretreatment technologies, including mechanical treatment [4], thermal treatment [5], chemical hydrolysis [6], electric fields [7, 8], enzymatic hydrolysis [9], and their combinations, were reported [10]. Previous studies showed that macroalgae hydrolysates can be used to produce acetone [11], butanol [11], ethanol [11], 1,2-propanediol [11], polyhydroxyalkanoates [12], succinic acid [13], extracellular polysaccharides, and biogas [14]. Although macroalgae complex carbohydrates can be effectively hydrolyzed with acid [6] or enzymatic catalysis [15] efficiently, these processes either require handling of large volumes of chemical waste [16] or are too expensive if the final products of fermentation are low-cost commodities such as fuels [15]. An alternative, green chemistry-directed solution for complex macroalgae carbohydrates deconstruction is subcritical thermal hydrolysis.

Electronic supplementary material The online version of this article (<https://doi.org/10.1007/s12155-019-10034-5>) contains supplementary material, which is available to authorized users.

✉ Alexander Golberg
agolberg@tauex.tau.ac.il

- ¹ Porter School of Environment and Earth Sciences, Tel Aviv University, Tel Aviv, Israel
- ² School of Mechanical Engineering, Tel Aviv University, Tel Aviv, Israel
- ³ The National Center for Mariculture, Israel Oceanographic and Limnological Research Ltd., Eilat, Israel
- ⁴ Mechanical Systems Design Department, Engineering Division, The Israel Electric Corporation, Haifa, Israel
- ⁵ School of Chemistry, Tel Aviv University, Tel Aviv, Israel

Subcritical hydrolysis uses water at subcritical temperatures (100–374 °C) as a solvent and a catalyst [17]. At temperatures near the critical point (374 °C), water becomes a poor dielectric, bad solvent for electrolytes, becomes compressible, expandable, and dissolves organic molecules. These new properties of water also make it a catalyst for biomass hydrolysis. At each reaction temperature in this range, the products of biomass hydrolysis include all three phases: solids, liquid, and gases. Reaction temperature around 180 °C leads to hydrothermal carbonization (HTC) with minimum gas production [17]. In this process, water molecules are released from the carbohydrates, leaving a solid residue with higher carbon fraction (hydrochar) and higher calorific value. A further increase of the temperature leads to an increase in the portion of liquid products and gases; above 374 °C gases are the major fraction of the reaction products. In addition to hydrochar, the breaking of biomass polysaccharides is expected to produce fragments with different lengths, including monosaccharides [18] which can be used as carbon sources for fermentation in the following steps. However, the released monosaccharides can further degrade in the high-temperature water environment into fermentation inhibiting products such

as formic acid, lactic acid, acetic acid, 5-hydroxymethylfurfural (5-HMF) [19], and levulinic acid [18]. Thus, there is a need to determine the impact of each process component on the fermentable monosaccharides released from the complex seaweed carbohydrates.

In parallel with the release of sugars and other metabolites from the biomass, residual organic is concentrated and transformed through the HTC process [20]. Many studies have been made in converting biomass and biomass waste [21] into hydrochar and in recent years, studies have been made on carbonization of macroalgae. These studies show that increasing temperature, the HHV increases and the hydrochar yield decreases. At 200 °C the high heat value (HHV) gain is 6–10.7 MJ kg⁻¹ compared with the initial biomass. Comparing the total heat that can be produced by combusting a biomass unit with the hydrochar that was produced from this biomass unit, a total of 33–60% of the combustion heat is lost. Although the total combustion heat is lost, the hydrochar energy density is increased, and most of the volatiles are removed, which makes it more suitable for co-combustion with coal than untreated biomass [22]. Table 1 summarizes studies on macroalgae hydrothermal treatments in recent years.

Table 1 Published data on subcritical hydrothermal treatments on macroalgae

Species	Parameters	Results	Reference
<i>Ulva pertusa</i>	100–200 °C and reaction times of 2–12 min	Maximum glucose yield of 8.5% (w/w) at 180 °C, 10.48 bar and 8 min reaction time	Choi et al. (2013) [23]
<i>Codium fragile</i>	100–240 °C and 10 min of residence time[24]	Soluble sugar production began at 170 °C and grew with temperature until a maximum was reached at 210 °C where more than 50% (w/w) was converted into soluble sugars. Further increase in temperature decreased soluble sugar yield with 7% (w/w) obtained at 240 °C. High heat value (HHV) of the solid residue increased constantly between 140 and 230 °C, until a maximum of 22.6 MJ kg ⁻¹ , an increase of 6 MJ kg ⁻¹ compared with the HHV of untreated biomass	Daneshvar et al. (2012) [24]
<i>Laminaria digitate</i> <i>Laminaria hyperborean</i> <i>Alaria esculenta</i>	The batch reactor at temperatures of 200 °C and 250 °C at the respective isobaric pressures of 16 and 40 bar	The hydrochar yield (w/w) was 22–39% at 200 °C and 18–32% at 250 °C. The char HHV increased from 11–14 to 21–23 MJ kg ⁻¹ at 200 °C and to 22.6–26.5 MJ kg ⁻¹ at 250 °C.	Smith and Ross (2016) [25]
Marine <i>Ulva</i> , <i>Derbesia</i> , <i>Chaetomorpha</i> , and <i>Cladophora</i> fresh water <i>Oedogonium</i> and <i>Cladophora</i>	Temperatures of 330–341 °C and pressures of 140–170 bar, for 5 min	HHV of 4–20.5 MJ kg ⁻¹ for the hydrochar and 32.5–33.8 MJ kg ⁻¹ for the bio-oil. Highest hydrochar HHV was measured for <i>Chaetomorpha</i> , while bio-oil HHV had no significant differences between species	Neveux et al. (2014) [26]
<i>Enteromorpha prolifera</i>	Temperatures of 220–320 °C	The bio-oil yield increased with temperature until a maximum of 20.4% (w/w) and HHV of 28.7 MJ kg ⁻¹ at 300 °C.	Zhou et al. (2010) [27]
<i>Laminaria japonica</i>	Temperatures of 220–280 °C Pressures 23–60 bar Residence time 28–42 min	The maximum yield of 814.10 mg reduced sugars/100 g raw dried algae sample at 200 °C, adding 1% acetic acid as catalyst.	Park et al. (2012) [28]
<i>Saccharina japonica</i>	Temperatures 180–260 °C, with a ratio solid load of 4% (w/w)	Glucose recovery was highest at 180 °C where 1.11 (g glucose/100 g dried algae sample) was recovered and lowest at 260 °C with 0.55 (g glucose/100 g dried algae sample) glucose recovery.	Meillisa et al. (2015) [18]

Past work on subcritical hydrolysis of macroalgae has produced only a partial description of the process. The reaction yield was presented for glucose [18, 23], xylose [23], and total sugars [24, 28], but not other monosaccharides that may be present as reaction products. The yield and properties were also investigated for the solid hydrochar [24–26] and the liquid biocrude [26, 27] products. However, to the best of our knowledge, co-production of fermentable monosaccharides and hydrochar was not reported. The degradation of sugars into undesired by-products that may inhibit fermentation such as 5-HMF was given only marginal consideration [23]. The impact of reaction temperature was widely investigated in all reported work, but other process parameters such as residence time were investigated only in a few cases [23]. Studies on the pH impact showed that the formation of organic acids decreases the pH but has no influence on the reaction rate [29]. The effect of biomass loading (mass fraction in water) was not studied. The effect of salinity was not studied, and in some cases, much of the naturally occurring salts were removed before the reaction [24]. The published knowledge on subcritical hydrolysis of macroalgae is then incomplete, since the impact and relative significance of various process parameters are only partly understood, and only some of the important reaction products were investigated.

The goal of this study was to develop a novel process for co-production of fermentable monosaccharides and hydrochar from macroalgae biomass with subcritical hydrolysis. To achieve this goal, the relative impact of four process parameters (temperature, treatment time, solid load, and salinity) on the release of a broad range of fermentable monosaccharides (glucose, xylose, rhamnose, fructose, and galactose) was determined in addition to the formation of the fermentation inhibitor 5-HMF. The study was done with *Ulva* sp., which is a green cosmopolitan seaweed that can be grown in multiple locations in the world [30]. Our previous work on Eastern Mediterranean *Ulva* sp. showed that it contains mostly glucose and rhamnose [31]. It is considered for multiple biorefinery applications [11]. The amount and the caloric value of the formed hydrochar for the optimum hydrolysis conditions were also determined. This study is significant as it provides detailed information on the impact of process parameters on the released from *Ulva* biomass monosaccharides coupled to the production of hydrochar. The detailed quantification of monosaccharides is important as it predicates the fermentation outcome [2].

Materials and Methods

Macroalgae Biomass Production

Green macroalgae *Ulva* sp., collected from a shore in Haifa, Israel, identified morphologically in ref [31], was grown under

controlled conditions using macroalgae photobioreactors (MPBR) incorporated in a building's south wall under daylight conditions, from September 15 to November 3, 2016 (Fig. 1). The detailed description of the cultivation system appears in ref [32]. Nutrients were supplied by adding ammonium nitrate (NH_4NO_3) and phosphoric acid (H_3PO_4) (Haifa Chemicals Ltd., IS) to maintain 6.4 g m^{-3} of total nitrogen and 0.97 g m^{-3} of total phosphorus in the seawater. The sole CO_2 source was bubbled air. Other conditions such as pH (8.2), salinity, and air flow rate (2–4 L/min) were maintained steady in all the reactors. The biomass was dried at $40 \text{ }^\circ\text{C}$ to constant weight.

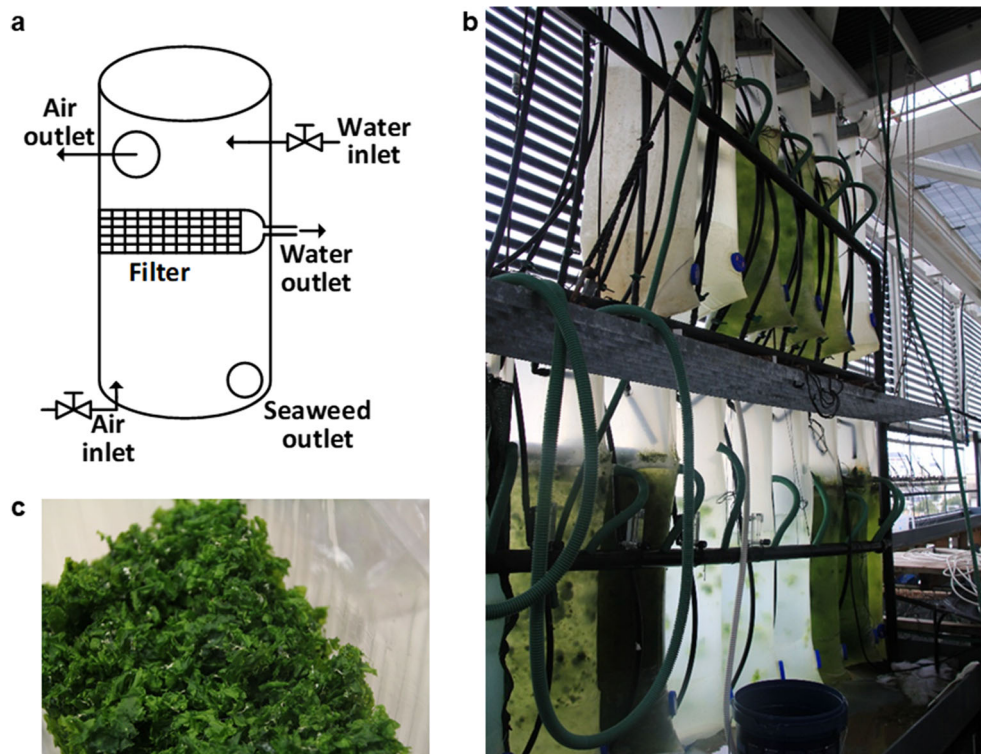
Subcritical Thermal Hydrolysis Experimental Setup

The batch experimental system that was used for biomass subcritical hydrothermal treatment is shown in Fig. 2. The 0.25-L batch reactor is heated by an electric heater (model C/JF-0.25 from Keda Machinery, China). The temperature is measured with an MRC TM-5005 digital temperature gauge using “Watlow 1/16” thermocouple type K. The heating rate was $\sim 5 \text{ }^\circ\text{C min}^{-1}$. The pressure is measured using “MRC PS-9302” pressure gauge with “MRC PS100-50BAR” sensor. A stirrer with water-cooled magnetic coupling drive was used to mix the slurry inside the pressure reactor. The reactor has 2 gas sampling ports and 1 liquid sampling line. The liquid line is equipped with a water-cooled condenser and a cold trap, before entering the sampling tube. The gas line is connected to a water-cooled condenser and a cold trap before reaching the sampling bag. The cooling water is circulated from a chiller (Guangzhou Teyu Electromechanical Co., Ltd. Cw-5200ai, China). Vacuum pump (MRC ST-85) is used to evacuate the air in the system before each experiment. The hydrolysate was separated to liquid and solid phases by centrifugation, 10,000 RPM for 3 min (Hettich Rotanta 46 RSC, Switzerland). The pH of the liquid phase was measured.

Taguchi Orthogonal Methodology for Subcritical Hydrolysis Optimization

The goal in these experiments was to determine the effects of subcritical water hydrolysis process parameters (temperature, treatment time, salinity (controlled by adding the required amount of sea salt (Red Sea Salt, Cheddar, UK) to the deionized water)) and solid loading on the release of monosaccharides from the *Ulva* sp. biomass. Pressure was excluded as previous studies already showed that it plays an insignificant role compared with other tested parameters [33]. The possible range of process parameters and their combinations is large. Therefore, to decrease the number of experiments, but still be able to evaluate the impact of each parameter independently, the Taguchi Robust Design method for the experimental design [34] was applied. This approach has advantages as it is a

Fig. 1 Macroalgae *Ulva* sp. cultivation in MPBR. **a** Schematic design of a single cultivation sleeve. **b** Digital image of the 29 cultivation sleeves. **c** Digital image of the produced *Ulva* sp. biomass



relatively simple method, requires a lower number of tests, flexible with few parameters, very robust method, and suitable for early process development phase or validation phase. Previous works verified the use of Taguchi approach for the optimization of process engineering parameters [35].

A key feature of the Taguchi method is the design of the experiment where process factors are tested with orthogonal

arrays. This design allows for the follow-up analysis that prioritizes the comparative impact of the process parameters on the yields. The tested parameters and their levels are shown in Table 2.

The experiments, conducted for the L9 orthogonal Taguchi array, which are needed to determine the individual effects of each of the tested parameters on the deconstruction yields are

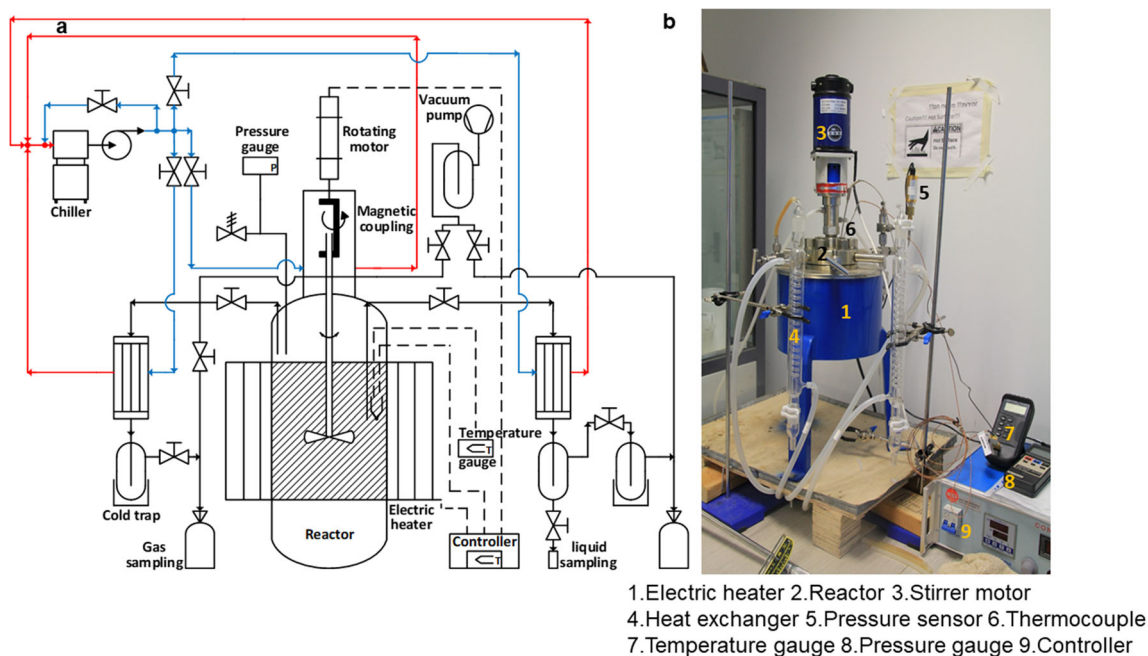


Fig. 2 Subcritical hydrolysis reactor. **a** Process flow diagram. **b** Digital image of the system. Major components are indicated

shown in Table S1. The experiments were conducted in two separate experimental blocks.

In Taguchi design of the experiment algorithm, the best parameter setting is determined using the signal-to-noise ratio (SN). In the experiments, the algorithm of “the larger the better” type was used. The ratio SN is determined independently for each of the process outcomes (OUT_max) that are optimized. In this study, the process outcomes are concentrations of glucose, rhamnose, galactose, xylose, fructose acid, and total sugars. In the current context, maximizing SN corresponds to obtaining the maximum concentration and extraction yields of monosaccharides. The ratio SN of a specific process outcome OUT in experiment j was calculated by:

$$SN^{OUT_max}(j) = -10 \times \log \left[\frac{1}{\#Reps} \sum_{Rep=1}^{\#Reps} \frac{1}{(m_{Rep})^2} \right] \quad 1 \leq j \leq K \quad (1)$$

where K is the number of experiments (in our case, K = 9; #Reps is the number of experiment repetitions, in our case, #Reps = 2) and m_{Rep} is the measurement of the process outcome (OUT) in the specific repetition Rep of experiment j.

When the process condition is optimized for reducing the concentration of produced toxic substances (OUT_min), for example, 5-HMF, “the smaller the better” type algorithm is used. In this case, the ratio SN of a specific process outcome OUT in experiment j was calculated by:

$$SN^{OUT_min}(j) = -10 \times \log \left[\frac{1}{\#Reps} \sum_{Rep=1}^{\#Reps} (m_{Rep})^2 \right] \quad 1 \leq j \leq K \quad (2)$$

Considering a process parameter P (temperature, treatment time, salinity, and solid loading as appears in Table 1) and assuming that P has a value of L in n(P,L) experiments (i.e., temperature = 170 appears in 3 experiments: P = temperature, L = 170, and n = 3). Let J(P, L) be the set of experiments in which process parameter P was applied at level L. Let:

$$SN^{OUT}(P, L) = \frac{1}{n(P, L)} \sum_{j \in J(P, L)} SN^{OUT}(j) \quad (3)$$

Table 2 Tested factors that affect biomass hydrolysis

Parameter	Level		
	1	2	3
Temperature (°C)	170	187	205
Residence time (min)	20	40	60
Solid loading (% dry algae weight/total mixture weight)	2	5	8
Salinity (% of sea water, 100% = 38 g/L sea salts)	0	50	100

be the average ratio SN for concrete level L of parameter P. The sensitivity (Δ) of each outcome (OUT) with respect to the change in a parameter P is calculated as:

$$\Delta^{OUT}(P) = Max\{SN^{OUT}(P, L)\} - Min\{SN^{OUT}(P, L)\} \quad (4)$$

Ranking (on the scale of 1–4, where 1 is the highest) was assigned to the process parameters according to the ranges obtained. The optimum parameter set was chosen according to maximal S/N

Severity Factor Calculation

The severity factor logR₀ (which incorporate temperature and time into one parameter) was also calculated for all experiments (Table 5) using the following correlation [36]

$$\log R_0 = \log \int_0^t \exp\left(\frac{T-100}{14.75}\right) dt \quad (5)$$

where T is the reactor temperature (°C) and t (min) is the time of the experiment including the pre-heating period and the residence time.

Analysis of the Released Carbohydrates

For monosaccharide and 5-HMF analysis in hydrolysates, an aliquot was diluted 20 times in ultrapure water and filtered through a 0.22-μm syringe-filter (Millipore, USA) in HPLC vials (Thermo Fischer Scientific, MA, USA). Monosaccharide and 5-HMF content in the hydrolysates were monitored by HPAEC-PAD (High-Pressure Anion-Exchange Chromatography coupled with Pulsed Amperometric Detection) using a Dionex ICS-5000 platform (Dionex, Thermo Fischer Scientific, MA, USA) with an analytical column (Aminopack 10) and its corresponding guard column. An electrochemical detector with an AgCl reference electrode was used for detection. The analysis was performed using an isocratic flow of 4.8 mM KOH generated by the Eluent Generator technology (Dionex, Thermo Fischer Scientific, MA, USA) for 20 min. Then the column was washed with 100 mM KOH between each run and re-equilibrated with 4.8 mM KOH prior to injection. The column temperature was kept at 30 °C, and the flow rate was set to 0.25 mL min⁻¹. Calibration curves were produced for each sugar with internal standards (Sigma, Israel). In this work, we quantified 5-HMF, rhamnose, galactose, glucose, xylose, and fructose.

The Mass Balance on the Hydrolysate Products

For mass balance analysis, first, the hydrolysate (H) was dried at 40 °C leading to solid matter (Z) that contained hydrochar, salts, and soluble solids. The mass of the evaporated water (E)

was measured gravimetrically. Second, the liquid phases (X) were sampled from the whole hydrolysate and dried at 40 °C (the mass of evaporated liquid (K) was measured gravimetrically as above). The resulted solids (T) contained salts and water-soluble organic matter. The total soluble solids (S) are calculated for the total hydrolysate volume. As the %salinity for the experiments is known, the total soluble ash-free solids (AFS) can be calculated as below.

$$\begin{aligned} H &= \text{Hydrochar} + E + T \\ T &= X - K \\ S &= (T/X) \times (X + E) \\ \text{AFS} &= S - (E + K) \times \% \text{salinity} \\ \text{Hydrochar} &= Z - S \end{aligned} \quad (6)$$

Elemental and Caloric Value Analysis

Elemental analysis was done at the Technion, Chemical, and Surface Analysis Laboratory using a Thermo Scientific CHNS Analyzer (Flash2000). The oxygen content was determined by the difference

$$\%O = 100\% - (\%C + \%H + \%N + \%S + \%Ash) \quad (7)$$

For caloric value and ash analysis, 2 g (DW) of untreated algae and residual carbonized material was dried at 40 °C to constant weight and was analyzed for energy content in HHV according to ASTM D5865–13 (Standard Test Method for Gross Calorific Value of Coal and Coke) and for ash according to D5142 standard by a certified laboratory of Israel Electric company. The adjusted HHV (same ash content as initial biomass) for the hydrochar was calculated according to:

$$\begin{aligned} \text{Adjusted HHV} &= \text{HHV}(\text{measured}) \\ &\times \left(\frac{1 - (\% \text{ash untreated } Ulva / 100)}{1 - (\% \text{ash after washing} / 100)} \right) \end{aligned} \quad (8)$$

Starch Analysis

The algae were grounded to a fine powder using a mortar and pestle with the help of liquid nitrogen and starch content was determined using a total starch assay kit (K-TSTA-100A, Megazyme, Ireland) according to AACC Method 76-13.01.

Fourier-Transform Infrared Spectroscopy

FT-IR spectroscopy analyses were performed on a Bruker Tensor 27 FT-IR spectrophotometer, equipped with standard Pike ATR attachment. FT-IR spectra of vacuum-dried *Ulva* algae biomass and corresponding biochar samples were measured in the spectral range of 4000–400 cm^{-1} (at 4 cm^{-1} resolution).

Differential Scanning Calorimetry and Thermogravimetric Analyses

Differential scanning calorimetry (DSC) and thermogravimetric (TG) analyses were performed in alumina ceramic pans on Netzsch STA 449 F5 Jupiter DSC-TG simultaneous analyzer, under flow of pure nitrogen gas (N_2 , 99.99%) and separately, under flow of a synthetic air (comprised 15% oxygen of 99.5% purity and 85% N_2 of 99.99% purity) at a flow rate of 70 mL min^{-1} (dynamic atmosphere). Typical samples of 3–4 mg were heated from 30 to 800 °C, at a heating rate of 10 °C min^{-1} .

Scanning Electron Microscopy

Samples were mounted on aluminum stubs and sputter-coated with gold (SC7620, Quorum). Images were captured on the scanning electron microscope (SEM) (JCM-6000, JEOL).

Statistical Analysis

Statistical analysis was performed with Excel (ver. 13, Microsoft, WA) Data analysis package and MATLAB software (ver. R2017a., MathWorks, Boston, MA). Standard deviation (\pm STDEV) is shown in error bars. At least two technical replicates were done for each experimental condition.

Results and Discussion

Green macroalgae *Ulva* sp. biomass major polymer composition includes cellulose (with glucose monomers), hemicellulose (xylose, galactose, rhamnose, and sometimes other monosaccharides as monomers), starch (with glucose monomers), ulvan (with rhamnose/glucuronic acid monomers), and proteins (with amino acids as monomers) [31]. Therefore, hydrolysis of whole *Ulva* sp. biomass is expected to release these monomers to the hydrolysate solution. Further dehydration of hexoses and pentoses leads to the formation of HMF and furfurals, respectively [37]. These are interesting by-products if separated downstream of the reactor, but can play a negative role as a fermentation inhibitor, if produced and not separated. The temperature/time plots for all experiments are shown in Fig. S1 (Supplementary Information). The reactor cooling down time was between 2 and 2.5 h until it reached room temperature. The actual treatment parameters for all 18 experiments are shown in Table S2. The pH of the hydrolysates was 3.

Glucose was the major released monosaccharide from *Ulva* sp. biomass under the tested conditions. The maximum yield achieved was 4.92 ± 0.73 mg glucose/g dry algae (Table 3 exp nos. 4 and 13), when 187 °C, 2% solid loading, 40 min residence time, and 100% salinity were used. Taguchi analysis

(Fig. 3(a), Table S3) showed that treatment temperature was the most important factor for maximum glucose yield, followed by salinity, then solid loading and residence time. In previous studies, at lower temperatures (100–134 °C) with acid catalyst, it showed that acid was the major factor that affected glucose release, followed by solid loading and then by time and temperature, which almost did not play a role in glucose release [3]. Comparing this result with an *Ulva* thermal hydrolysis study [23] shows a big difference with 8.5% glucose yield obtained at 180 °C, 8 min residence time, and 9% solid loading. The big difference may be attributed to the higher starch concentration in [23] with 4.5 times more starch than in this study (Table 3). An additional study that used a combination of hydrothermal treatment at 150 °C with enzyme hydrolysis was reported on the release of 11% glucose/g dry algae [38], showing that a future cost/benefit analysis of adding enzymes to the process is needed as enzymes significantly improved the yields. The more similar result was obtained compared with the study of *Saccharina japonica* [18] with 1.11% glucose yield at 180 °C; however, the carbohydrate content was not specified and differences in the studied algae could lead to a difference in the results.

The maximum average yield achieved for rhamnose, a rare sugar derived from the deconstruction of ulvan in this process, was 1.95 ± 1.05 mg rhamnose/g dry algae (Table 3 exp nos. 3 and 12), when 170 °C, 8% solid loading, 40 min residence time, and 100% salinity were used. Taguchi analysis (Fig.

3(b), Table S4) showed that the temperature was the most important factor for maximum glucose yield, followed by salinity, then solid loading and residence time. Our previous studies at lower temperatures (100–134 °C) with acid catalyst showed that acid was the major factor that affected rhamnose release, followed by solid loading and then by time and temperature, which almost did not play a role in rhamnose release [3]. A study that used a combination of hydrothermal treatment at 150 °C with enzyme hydrolysis reported on the release of 9% rhamnose/g dry algae [38].

The maximum average yield achieved for galactose, a sugar derived from the deconstruction of hemicellulose in this process, was 0.49 ± 0.01 mg galactose/g dry algae (Table 3 exp nos. 6 and 15), when 187 °C, 8% solid loading, 20 min residence time, and 50% salinity were used. Taguchi analysis (Fig. 3(c), Table S5) showed that temperature was the most important factor for maximum glucose yield, followed by salinity, then solid loading and residence time. A study that used a combination of hydrothermal treatment at 150 °C with enzyme hydrolysis reported on the release of 0.7% glucose/g dry algae [38]

The maximum yield achieved for xylose, a sugar derived from the deconstruction of hemicellulose in our process, was 1.48 ± 0.12 mg xylose/g dry algae (Table 3 exp nos. 3 and 12) when 170 °C, 8% solid loading, 60 min residence time, and 100% salinity were used. Taguchi analysis (Fig. 3(d), Table S6) showed that temperature was the most important

Table 3 Measured products from subcritical hydrolysis of *Ulva* sp. in experimental conditions as shown in Table 2. No arabinose was detected in any sample

Exp no.	T (°C)	Time (min)	Log R ₀ (severity)	Glucose mg/gDW	Rhamnose mg/gDW	Galactose mg/gDW	Xylose mg/gDW	Fructose mg/gDW	Total yield	HMF
1	170	20	3.48	2.02	1.13	0	1	1.69	5.84	0
2	170	40	3.67	1.37	0.93	0.02	0.94	0.74	4.00	0.16
3	170	60	3.9	6.11	0.9	0.5	1.36	1.27	10.14	1.3
4	187	40	4.16	4.19	1.7	0.41	0.6	1.15	8.05	2.3
5	187	60	4.38	2.43	0.09	0.1	0	0.95	3.57	2.58
6	187	20	3.96	1.45	0.97	0.5	0.65	0.42	3.99	0.72
7	205	60	4.88	0	0	0	0	0	0.00	3.5
8	205	20	4.34	2.12	0	0.01	0	0.82	2.95	4.22
9	205	40	4.62	0.21	0	0	0	0	0.21	2
10	170	20	3.53	2.76	0.98	0	1	2.35	7.09	0
11	170	40	3.68	1.22	1.35	0.1	0.93	0.81	4.41	0.58
12	170	60	3.84	2.67	3	0.46	1.6	0.78	8.51	1.31
13	187	40	4.22	5.64	2	0.33	0.62	1.93	10.52	5
14	187	60	4.38	2.22	0.32	0.04	0	0.88	3.46	3
15	187	20	4.06	5.77	1.8	0.48	0.57	1.62	10.24	3.77
16	205	60	4.85	0	0	0	0	0	0.00	0
17	205	20	4.29	2.57	0	0	0.22	1.1	3.89	9.45
18	205	40	4.62	0.1	0	0	0	0.03	0.13	3.2

factor for maximum glucose yield, followed by salinity, then solid loading and residence time. Previous studies at lower temperatures (100–134 °C) with acid catalyst showed that acid was the major factor that affected xylose release, followed by solid loading and then by time and temperature, which almost did not play a role in xylose release [3]. A study that used a combination of hydrothermal treatment at 150 °C with enzyme hydrolysis reported on the release of 2.9% glucose/g dry algae [38]

The maximum yield achieved for fructose, a sugar that could be derived from isomerization of glucose released from the deconstruction of cellulose and starch in our process, was 1.54 ± 0.39 mg fructose/g dry algae (Table 3 exp nos. 4 and 13), when 187 °C, 2% solid loading, 40 min residence time, and 100% salinity were used. Taguchi analysis (Fig. 3(e), Table S7) showed that temperature was the most important

factor for maximum fructose yield, followed by salinity, then solid loading and residence time.

The optimum parameters for the maximum monosaccharides release under the lowest 5-HMF constrain are shown in Table 4. The minimum yield of produced 5-HMF, potentially corresponding to the minimum toxicity of the hydrolysate for subsequent fermentation, was 0 mg HMF/g dry algae (Table 3 exp nos. 1 and 10), when 170 °C, 2% solid loading, 20 min residence time, and 0% salinity were used. Taguchi analysis (Fig. 3(f), Table S8) showed that temperature was the most important factor for minimum HMF yield, followed by residence time, then salinity and solid loading. The optimum parameters for the minimum HMF production were determined as 170 °C, 2% solid loading, 20 min residence time, and 0% salinity (Table 4). The maximum concentration of HMF, 6.83 ± 2.61 mgHMF/g dry algae, was detected at experiments 8

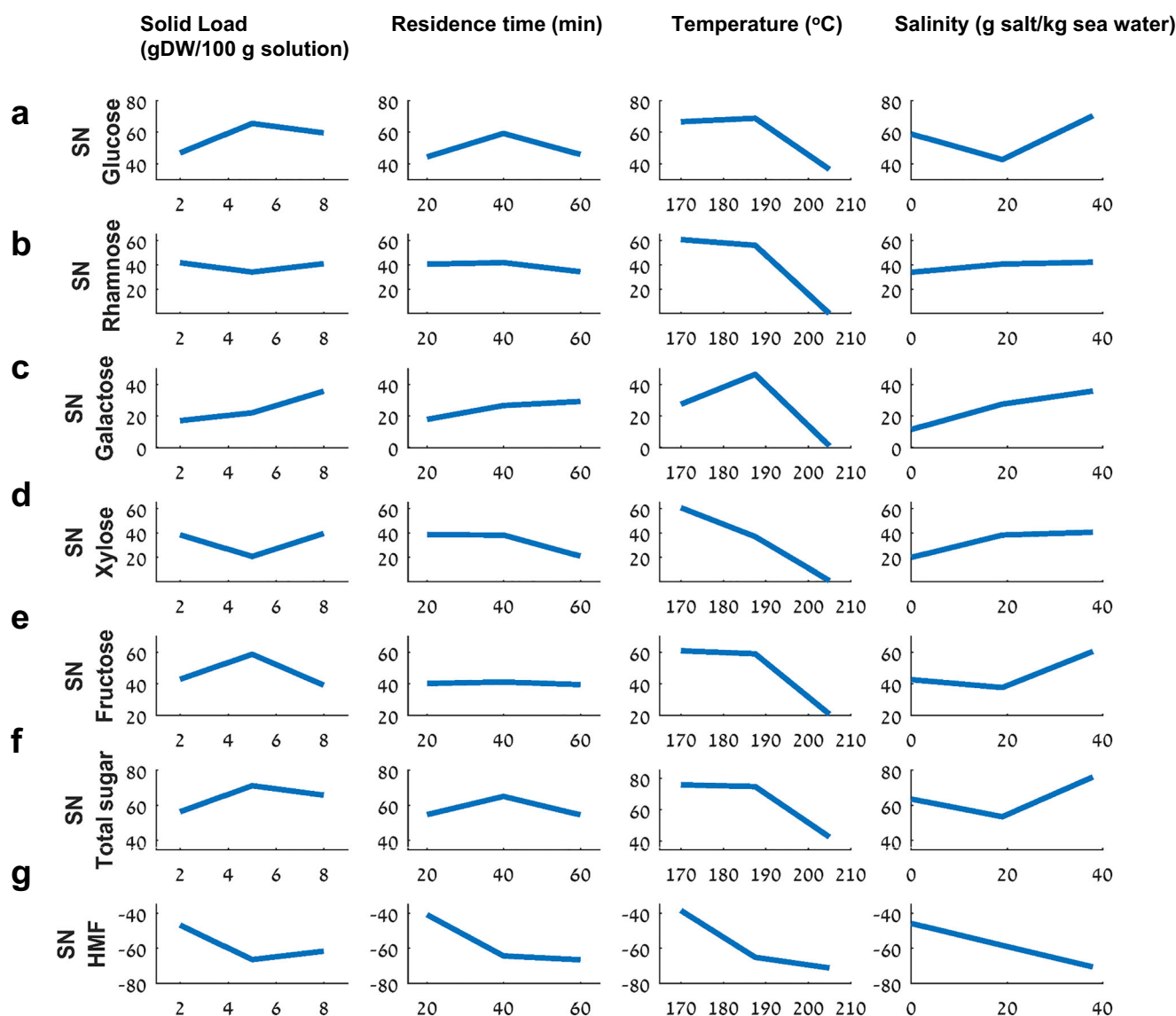


Fig. 3 Taguchi signal-to-noise (SN) analysis of process parameters on product release. (a) glucose, (b) rhamnose, (c) galactose, (d) xylose, (e) fructose, (f) HMF, (g) total monosaccharides

Table 4 Optimum process conditions for maximum monosaccharide release and minimum HMF production by subcritical water hydrolysis in the range of parameters as defined in Table 2

	Temp (°C)	Time (min)	Solid loading %	Salinity %
Rhamnose	170	40	2	100
Galactose	187	60	8	100
Glucose	187	40	8	100
Xylose	170	20	8	100
Fructose	170	40	5	100
HMF	170	20	2	0
Total monosaccharides	170	40	5	100

and 17, when 205 °C, 5% solid loading, 20 min residence time, and 100% salinity were applied (Table 3). This is equivalent to 341.5 ± 130.5 mgHMF/L of hydrolysate, which is lower than reported levels of HMF (1–15 g/L) that inhibit growth and ethanol fermentation of different strains of *Saccharomyces cerevisiae* [39].

The maximum total sugar yield was 9.34 ± 0.81 mg sugars/g dry algae (Table 3 exp nos. 3 and 12), when 170 °C, 8% solid loading, 60 min residence time, and 100% salinity were used. At these conditions, 1.3 ± 0.1 mgHMF/g dry algae were detected (Table 3). This yield is lower than that reported in previous studies that used various catalysis hydrolysis, which in some studies led to more than 200 mg sugars/g dry algae [4, 40, 41]. Future economic and environmental impact analysis is needed to compare the costs and benefits of these yields

increased with harsh chemicals and enzymes. The maximum yield was achieved at the R_0 of 3.8–4.2 (Fig. S2, Table 3) and rapidly decreased at R_0 higher than 4.4. The highest HMF was observed at R_0 4.1–4.3 (Fig. S2, Table 3). Similar results were previously observed for *Ulva intestinalis* [42].

Taguchi analysis (Fig. 3(g), Table S9) showed that temperature was the most important factor for maximum total sugars yield, followed by salinity, then solid loading and residence time. This difference between the importance of temperature (the most important parameter) and residence time (the least important parameter) could potentially explain the high scatter of total yield vs R_0 (Fig. S2), suggesting that the commonly used severity factor, which includes both temperature and time, should not be a good predictor of performance. Similar results have been observed in high-voltage pulsed electric field treatment of bacteria and food. In this type of treatment, electric field strength plays a more important role in the process than pulse duration and a number of pulses, and, therefore, total delivered energy is not a useful predictor of the performance [43] and reporting of individual parameters is recommended by the expert panel [44] (Fig. 4).

Previous studies at lower temperatures (100–134 °C) with acid catalyst showed that acid was the major factor that affected total release, followed by solid loading and then by time and temperature, which almost did not play a role in the total sugar release [3]. The results also show that increasing the temperature and residence time above certain values (specific for each sugar Fig. 2) led to a decrease in sugar concentrations. However, the increase in temperature and time led to an increase of HMF formation. These results are

Fig. 4 Digital image and caloric value of the dried *Ulva* sp. biomass before (a) and after (b) subcritical hydrolysis (hydrochar). c The liquid fraction of the hydrolysate. d Proximate analysis, ash, and caloric value of the untreated biomass and hydrochar after hydrothermal treatment. C, H, N, S, and O, are the weight percentage of carbon, hydrogen, nitrogen, sulfur, and oxygen respectively

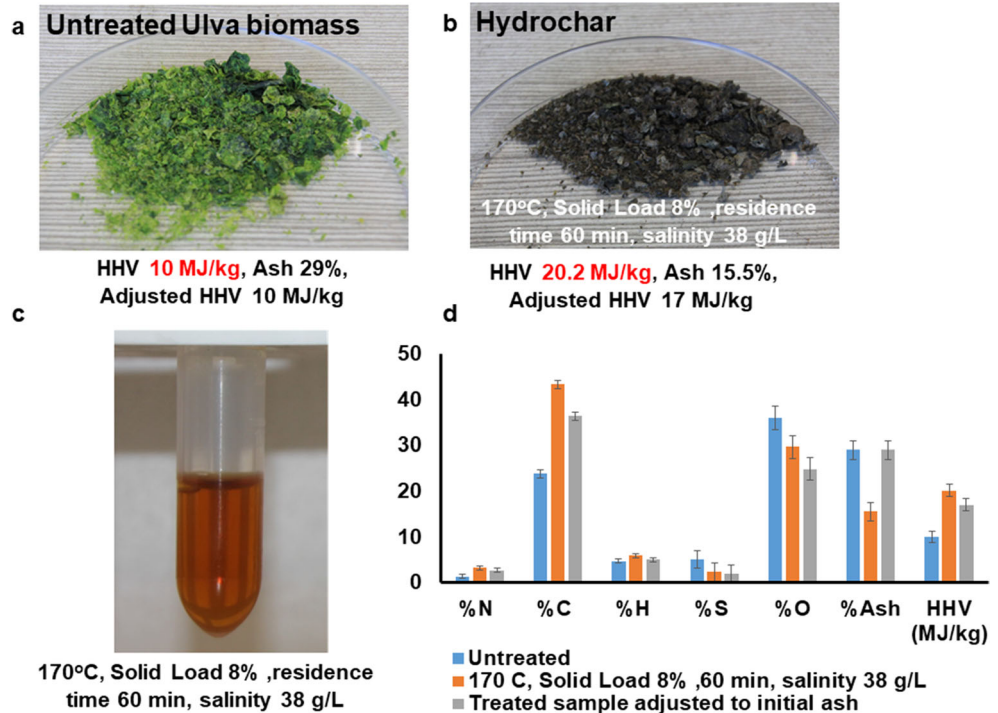
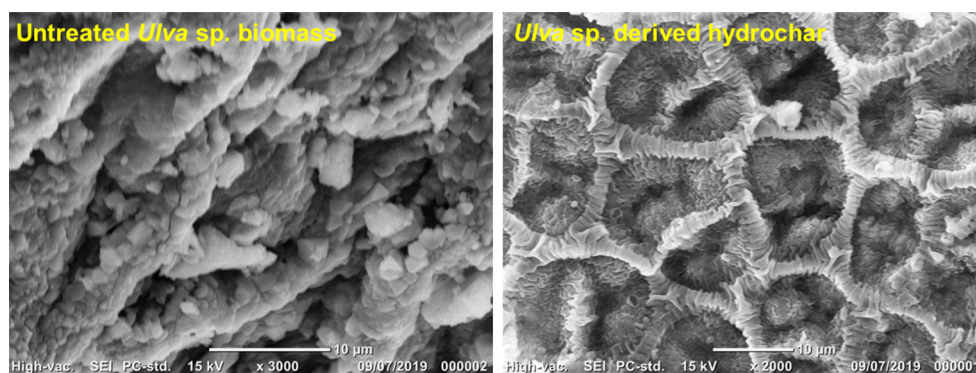


Fig. 5 Scanning electron microscopy of the untreated *Ulva* sp. biomass (left) and hydrochar produced at 170 °C, solid load 8%, residence time 60 min, and salinity 38 g/L (right)



consistent with previous reports on the HMF formation from partial hexose degradation [45]. It is important to note that previous studies also showed isomerization of monosaccharides under subcritical water treatment [46], a process which can affect the availability of the products for fermentation. Importantly, the heating and cooling rates affect the kinetics of chemical transformations observed, and thus, different reactor designs could lead to different outcome chemistry of the products [47].

For the experimental conditions with the highest total monosaccharides yields, the solid residue was characterized (Fig. 5), which could be used for direct combustion (Table 5). It was found that at 170 °C, solid loading 8%, residence time 60 min, and salinity of 100%, the macroalgae hydrochar yield (wt/wt) was $19.4 \pm 3\%$, the water-soluble solids yield were $58.2 \pm 3.2\%$ with moisture release of 19.1%, and the rest of the 3.3% can be attributed to produced volatiles and/or water formation during the carbonization process. The mass balance for the hydrolysis products appears in Table 6. The hydrochar

HHV obtained was 20.2 MJ/kg, or adjusted HHV of 17 MJ/kg (with hydrochar containing 15.5 wt% ashes). The ultimate, proximate, starch, and HHV are summarized in Table 5.

The hydrochar carbon content increased and oxygen content decreased compared with the original biomass due to the carbonization process thus increasing the HHV by 9–10 MJ (energy densification of 1.85–2) compared with the initial sample. The energy yield (energy densification multiplied by hydrochar yield) is 42–46%, similar to other carbonization studies on macroalgae which show 40–67% energy yield [50]. The current results further corroborate the previous work on macroalgae hydrothermal carbonization (HHV increase from 10 ± 0.02 HHV to 20.2 ± 1.31 HHV (Fig. 5)). Previous hydrothermal carbonization work on a brown seaweed *Sargassum horneri* increased the HHV of the biomass from 17.4 MJ/kg in the untreated biomass to 25.1 MJ/kg under 16 h treatment with 5% solid loading, 210 °C, 0.04% citric acid catalyst [50]. In another work, carbonization of a brown seaweed (unidentified) collected from natural stocks was done at 900 °C and a heating rate of 10 °C/min. Although the carbon % increased from 42.7 to 84.8%, the heating value increased from 12.5 to 14.3 MJ/kg, indicating that elimination of volatiles at this temperature leads to the decrease of the heating value [51]. Hydrothermal carbonization of three kelps *Laminaria digitata*, *Laminaria hyperborea*, and *Alaria esculenta* at 250 °C increased the caloric value from 11.4 to

Table 5 *Ulva* sp. biomass and hydrochar properties

		Untreated seaweed biomass	Hydrochar (170 °C), solid loading (8%, 40 min), salinity (38 g/L)
Ultimate (wt%)	N (%)	1.3	3.2
	C (%)	23.8	43.3
	H (%)	4.7	6.2
	S (%)	5.1	1.2
	O (%)	36	30.4
Proximate (wt%)	Ash	29	15.5
	Moisture	20.6	7.5
Biochemical (wt%)	Starch	4.4	–
HHV (MJ kg ⁻¹)	Boie [48]	10.5	19.4
	Grummel and Davis [49]	9.6	18.7
	Measured value (calorimeter)	10 ± 0.02	20.2 ± 1.31

Table 6 *Ulva* sp. biomass hydrolysate mass balance for hydrolysis done with 170 °C; solid loading 8%, 40 min; and salinity 38 g/L. Drying was done at 40 °C

Product	A fraction from the total initial mass (%)
Hydrochar, ash-free	19.4
Water-soluble solids, ash-free (AFS)	58.2
Moisture	19.1
Highly volatile molecules + water produced during HTC	3.3
Total	100

Table 7 Wavenumbers and attributed function groups and their vibration modes relevant to *Ulva* algae biomass and corresponding biochar

	Wavenumber (cm ⁻¹)	Functional group and vibration mode
1.	3600–3000	Stretching of O–H bonds in carboxylic acids and alcohols
2.	3000–2800	Asymmetric and symmetric stretching of aliphatic C–H bonds
3.	1700	Stretching of aldehydes and ketones C=O bonds
4.	1500–1600	Bending and stretching of aromatic C–C bonds
5.	1400–1500	Deformation C–H bonds in alkene groups
6.	1200–1300, 1000–1100	Stretching of C–O bonds in alkyl and aryl ethers
7.	850–900	Bending out of the plane of aromatic C–H bonds
8.	650–750	Bending in the plane of alkenes C=C bonds

22.6 MJ/kg, 11.2 to 24.1 MJ/kg, and 12.8 to 24.7 MJ/kg, respectively [25].

Scanning electron microscopy morphology of the hydrochar (Fig. 5) shows the formation of highly organized porous structures, similar to previous reports on hydrochar production other biomass [52].

The FT-IR spectroscopy of the hydrochar and untreated biomass is shown in Fig. S3. The IR bands assigned to relevant functional groups are summarized in Table 7. Analysis of both IR spectra (superimposed in Fig. S3) showed that the dry *Ulva* biomass prior to and after thermal treatment (the hydrochar) has a certain degree of similarity in their chemical compositions, showing common bands in most spectral regions. However, changes in intensities of specific bands indicate a relative increase in abundance of specific functional groups, which could be attributed to carbonization process that *Ulva* biomass underwent upon its thermal treatment and conversion to the corresponding hydrochar.

Major difference in peak intensities between two spectra was found in 3200–3300, 2900–2950, 1000–1100, and 846 cm⁻¹ regions that could be attributed to a significant increase in the number of O–H functional groups, measurable reduction in the number of aliphatic C–H bonds, peak sharpening and significant increase in the number of C–O bonds belonging to alkyl and aryl ethers, and appearance of aromatic C–H bonds in the biochar (which were not present in the *Ulva* biomass prior to the thermal treatment), respectively [53, 54]. All these changes clearly indicate that aromatic and polyaromatic phenols and ethers were formed during the carbonization of the *Ulva* biomass, which is consistent with chemistry of previous reports [55].

TG analysis of room temperature vacuum-dried *Ulva* biomass and the corresponding hydrochar allowed us to evaluate structural stability of these materials by monitoring their weight loss patterns, resulted from exposure to gradually elevated temperature, at a specific heating rate, and under controlled atmosphere. TG analyses showed differences between thermal decomposition of *Ulva* biomass and its hydrochar, under both N₂ and air-oxidizing atmospheres (Fig. S4).

Under N₂ atmosphere, a total decomposition (mass loss after heating to 800 °C) for *Ulva* biomass was in the range of 86%, while for the biochar, the mass loss was 74%. Under the air atmosphere, the mass losses for the *Ulva* biomass and for biochar were 76% and 73%, respectively (Fig. S4). For both materials (under N₂ and air atmospheres), three stages of decomposition were detected, which included dehydration, volatilization (thermal decomposition of cellulose and hemicellulose, in a range of 250–350 °C), and decomposition (corresponding to the decomposition of chars, carbonates, and other inorganic materials, at above 500 °C) that is in line with reports of other investigators [55]. The derivative TG thermograms (DTG; Fig. S4c, d) are showing the most significant mass loss temperature ranges for both analyzed materials and under both atmospheric conditions. The dehydration step (at peak temperature 93–96 °C) in both materials and under both atmospheric conditions was followed by the volatilization process, which, under N₂ atmosphere, took place in a temperature range of 202–221 °C (with mass loss of 9%), in the case of *Ulva* biomass, and in a range of 252–354 °C (with mass loss of 13%), in the case of hydrochar (Fig. S4a). While under air atmosphere, the volatilization process took place in a temperature range of 205–222 °C (with mass loss of 8%), in the case of *Ulva* biomass, and in a range of 253–349 °C (with mass loss of 19%), in the case of biochar (Fig. S4b). The subsequent decomposition process, under N₂ atmosphere, took place in a temperature range of 578–699 °C (with mass loss of 12%), in the case of *Ulva* biomass, and in a range of 593–740 °C (with mass loss of 11%), in the case of hydrochar (Fig. S4a). While under air atmosphere, the decomposition process took place in a temperature range of 526–599 °C (with mass loss of 14%), in the case of *Ulva* biomass, and in a range of 510–565 °C (with mass loss of 6%), in the case of hydrochar (Fig. S4b).

The temperature ranges of mass losses detected in TG (and DGT) thermograms are well correlated with the exothermic peaks observed in the corresponding DSC thermograms (Fig. S5). Under oxidizing air atmosphere, the exothermic peaks could be attributed to the thermal oxidation of cellulose and hemicellulose components (Fig. S5b). Indeed, under the air

atmosphere, DSC thermogram of *Ulva* biomass showed mostly two exothermic peaks, a minor peak, with a top temperature of 349 °C (proposed as oxidation process of aromatic moieties), and a major peak, with a top temperature of 554 °C. In contrast, in a hydrochar DSC thermogram, the heat release was more intense and two major peaks were observed at 328 °C and 533 °C, where the amount of released heat was larger around the peak at 328 °C, indicating that hydrochar could be potentially more advantageous as fuel than *Ulva* biomass. Under a N₂ atmosphere, below 700 °C, no relatively narrow peaks were detected, while observed broad heat-release behavior could be attributed to the thermal decomposition accompanied by oxidation (Fig. S5a).

Conclusions

In this study, a novel approach for co-production of fermentable monosaccharides and hydrochar from seaweed biomass with subcritical water treatment was developed. This study shows that subcritical water treatment of green macroalgae *Ulva* sp. biomass leads to the partial deconstruction of heterogeneous macroalgae to simple. In addition, 5-HMF is produced as a part of degradation reactions. The optimum parameters for the maximum total sugar release were determined as 170 °C (800 kPa abs.), 5% solid loading, 40 min residence time, and 100% salinity. Taguchi analysis indicated the temperature as the most important factor for maximum total sugar yield, followed by salinity, then solid loading and residence time. Higher reaction temperatures and long residence times lead to sugar degradation and formation of 5-HMF. In addition, it was found that treatment of *Ulva* sp. biomass at 170 °C, solid loading 8%, residence time 60 min, 100% salinity produced macroalgae hydrochar with 19.4% yield and HHV 20.2 ± 1.31 MJ/kg. It was shown that subcritical water can be used for co-production of macroalgae biomass into multiple monosaccharides and caloric-rich solid residue, both important for bioenergy generation.

Acknowledgments The authors sincerely thank Vered Holdengreber from the Electron Microscopy Unit, Inter-Departmental Research Facility Unit, Faculty of Life Sciences, Tel Aviv University, for the help with SEM.

Funding Information This study was financially supported by the Israeli Ministry of Energy, Infrastructures and Water Resources (grant no. 215-11-032).

Compliance with Ethical Standards

Conflict of Interest The authors declare that they have no conflict of interest.

References

1. Fernand F, Israel A, Skjermo J, Wichard T, Timmermans KR, Golberg A (2016) Offshore macroalgae biomass for bioenergy production: environmental aspects, technological achievements and challenges. *Renew Sustain Energy Rev* 75:35–45. <https://doi.org/10.1016/j.rser.2016.10.046>
2. Vitkin E, Golberg A, Yakhini Z (2015) BioLEGO — a web-based application for biorefinery design and evaluation of serial biomass fermentation. *Technology* 1–10. <https://doi.org/10.1142/S2339547815400038>
3. Jiang R, Linzon Y, Vitkin E, Yakhini Z, Chudnovsky A, Golberg A (2016) Thermochemical hydrolysis of macroalgae *Ulva* for biorefinery: Taguchi robust design method. *Sci Rep* 6. <https://doi.org/10.1038/srep27761>
4. Korzen L, Pulidindi IN, Israel A, Abelson A, Gedanken A (2015) Single step production of bioethanol from the seaweed *Ulva rigida* using sonication. *RSC Adv* 5:16223–16229. <https://doi.org/10.1039/C4RA14880K>
5. Jung H, Baek G, Kim J, Shin SG, Lee C (2015) Mild-temperature thermochemical pretreatment of green macroalgal biomass: effects on solubilization, methanation, and microbial community structure. *Bioresour Technol* 199:326–335. <https://doi.org/10.1016/j.biortech.2015.08.014>
6. Pezoa-Conte R, Leyton A, Anugwom I, von Schoultz S, Paranko J, Mäki-Arvela P, Willför S, Muszyński M, Nowicki J, Lienqueo ME, Mikkola JP (2015) Deconstruction of the green alga *Ulva rigida* in ionic liquids: closing the mass balance. *Algal Res* 12:262–273. <https://doi.org/10.1016/j.algal.2015.09.011>
7. Robin A, Golberg A (2016) Pulsed electric fields and electroporation technologies in marine macroalgae biorefineries. 1–16. https://doi.org/10.1007/978-3-319-26779-1_218-1
8. Robin A, Kazir M, Sack M, Israel A, Frey W, Mueller G, Livnev YD, Golberg A (2018) Functional protein concentrates extracted from the green marine macroalga *Ulva* sp., by high voltage pulsed electric fields and mechanical press. *ACS Sustain Chem Eng* 6: 13696–13705. <https://doi.org/10.1021/acssuschemeng.8b01089>
9. Powell B, Marquez G, Takeuchi H, Hasegawa T (2015) Biogas production of biologically and chemically-pretreated seaweed, *Ulva* spp., under different conditions: freshwater and thalassic. *J Japan Inst Energy*. <https://doi.org/10.3775/jie.94.1066>
10. Maneein S, Milledge JJ, Nielsen BV, Harvey PJ (2018) A review of seaweed pre-treatment methods for enhanced biofuel production by anaerobic digestion or fermentation. *Fermentation*. <https://doi.org/10.3390/fermentation4040100>
11. Bikker P, van Krimpen MMM, van Wikselaar P, et al. (2016) Biorefinery of the green seaweed *Ulva lactuca* to produce animal feed, chemicals and biofuels
12. Ghosh S, Gnaim R, Greiserman S, Fadeev L, Gozin M, Golberg A (2019) Macroalgal biomass subcritical hydrolysates for the production of polyhydroxyalkanoate (PHA) by *Haloferax mediterranei*. *Bioresour Technol* 271:166–173. <https://doi.org/10.1016/j.biortech.2018.09.108>
13. Olajuyin AM, Yang M, Liu Y, Mu T, Tian J, Adaramoye OA, Xing J (2016) Efficient production of succinic acid from *Palmaria palmata* hydrolysate by metabolically engineered *Escherichia coli*. *Bioresour Technol*. 214:653–659. <https://doi.org/10.1016/j.biortech.2016.04.117>
14. Ganesh Saratale R, Kumar G, Banu R, Xia A, Periyasamy S, Dattatraya Saratale G (2018) A critical review on anaerobic digestion of microalgae and macroalgae and co-digestion of biomass for enhanced methane generation. *Bioresour Technol* 262:319–332
15. Klein-Marcuschamer D, Oleskowicz-Popiel P, Simmons BA, Blanch HW (2012) The challenge of enzyme cost in the production

- of lignocellulosic biofuels. *Biotechnol Bioeng* 109:1083–1087. <https://doi.org/10.1002/bit.24370>
16. Sun ZY, Tang YQ, Morimura S, Kida K (2013) Reduction in environmental impact of sulfuric acid hydrolysis of bamboo for production of fuel ethanol. *Bioresour Technol* 128:87–93. <https://doi.org/10.1016/j.biortech.2012.10.082>
 17. Cocero MJ, Cabeza Á, Abad N, Adamovic T, Vaquerizo L, Martínez CM, Pazo-Cepeda MV (2018) Understanding biomass fractionation in subcritical & supercritical water. *J Supercrit Fluids* 133:550–565. <https://doi.org/10.1016/J.SUPFLU.2017.08.012>
 18. Meillisa A, Woo H-CC, Chun B-SS (2015) Production of mono-saccharides and bio-active compounds derived from marine polysaccharides using subcritical water hydrolysis. 171:70–77. <https://doi.org/10.1016/j.foodchem.2014.08.097>
 19. Mutripah S, Meinita MDN, Kang JY, Jeong GT, Susanto AB, Prabowo RE, Hong YK (2014) Bioethanol production from the hydrolysate of *Palmaria palmata* using sulfuric acid and fermentation with brewer's yeast. *J Appl Phycol* 26:687–693. <https://doi.org/10.1007/s10811-013-0068-6>
 20. Bergius FCR (1913) Anwendung hoher Drucke bei chemischen Vorgängen und die Nachbildung des Entstehungsprozesses der Steinkohle. Halle a.S., Knapp
 21. Wang T, Zhai Y, Zhu Y, Li C, Zeng G (2018) A review of the hydrothermal carbonization of biomass waste for hydrochar formation: process conditions, fundamentals, and physicochemical properties. *Renew Sust Energy Rev* 90:223–247. <https://doi.org/10.1016/j.rser.2018.03.071>
 22. Liu Z, Quek A, Hoekman SK et al (2012) Thermogravimetric investigation of hydrochar-lignite co-combustion. *Bioresour Technol* 123:646–652. <https://doi.org/10.1016/j.biortech.2012.06.063>
 23. Choi W-Y, Kang D-H, Lee H-Y (2013) Enhancement of the saccharification yields of *Ulva pertusa* Kjellmann and rape stems by the high-pressure steam pretreatment process. *Biotechnol Bioprocess Eng* 18:728–735. <https://doi.org/10.1007/s12257-013-0033-x>
 24. Daneshvar S, Salak F, Ishii T, Otsuka K (2012) Application of subcritical water for conversion of macroalgae to value-added materials. *Ind Eng Chem Res* 51:77–84. <https://doi.org/10.1021/ie201743x>
 25. Smith AM, Ross AB (2016) Production of bio-coal, bio-methane and fertilizer from seaweed via hydrothermal carbonisation. *Algal Res* 16:1–11. <https://doi.org/10.1016/j.algal.2016.02.026>
 26. Neveux N, Yuen AKL, Jazrawi C, Magnusson M, Haynes BS, Masters AF, Montoya A, Paul NA, Maschmeyer T, de Nys R (2014) Biocrude yield and productivity from the hydrothermal liquefaction of marine and freshwater green macroalgae. *Bioresour Technol* 155:334–341. <https://doi.org/10.1016/j.biortech.2013.12.083>
 27. Zhou D, Zhang L, Zhang S, Fu H, Chen J (2010) Hydrothermal liquefaction of macroalgae *Enteromorpha prolifera* to bio-oil. *Energy Fuels* 24:4054–4061. <https://doi.org/10.1021/ef100151h>
 28. Park J-N, Shin T-S, Lee J-H, Chun B-S (2012) Production of reducing sugars from *Laminaria japonica* by subcritical water hydrolysis. *APCBEE Proc* 2:17–21. <https://doi.org/10.1016/j.apcbee.2012.06.004>
 29. Bobleter O, Schwald W, Concin R, Binder H (1986) Hydrolysis of cellobiose in dilute sulfuric acid and under hydrothermal conditions. *J Carbohydr Chem* 5:387–399. <https://doi.org/10.1080/07328308608058843>
 30. Lehahn Y, Ingle KN, Golberg A (2016) Global potential of offshore and shallow waters macroalgal biorefineries to provide for food, chemicals and energy: feasibility and sustainability. *Algal Res* 17:150–160. <https://doi.org/10.1016/j.algal.2016.03.031>
 31. Robin A, Chavel P, Chemodanov A, Israel A, Golberg A (2017) Diversity of monosaccharides in marine macroalgae from the Eastern Mediterranean Sea. *Algal Res* 28:118–127. <https://doi.org/10.1016/j.algal.2017.10.005>
 32. Chemodanov A, Robin A, Golberg A (2017) Design of marine macroalgae photobioreactor integrated into building to support seagrass culture for biorefinery and bioeconomy. *Bioresour Technol* 241:1084–1093. <https://doi.org/10.1016/j.biortech.2017.06.061>
 33. Aida TM, Tajima K, Watanabe M, Saito Y, Kuroda K, Nonaka T, Hattori H, Smith RL Jr, Arai K (2007) Reactions of D-fructose in water at temperatures up to 400 °C and pressures up to 100 MPa. *J Supercrit Fluids* 42:110–119. <https://doi.org/10.1016/j.supflu.2006.12.017>
 34. Rao RS, Kumar CG, Prakasham RS, Hobbs PJ (2008) The Taguchi methodology as a statistical tool for biotechnological applications: a critical appraisal. *Biotechnol J* 3:510–523
 35. Rao RS, Prakasham RS, Prasad KK, et al. (2004) Xylitol production by *Candida* sp.: parameter optimization using Taguchi approach. *Process Biochem*. [https://doi.org/10.1016/S0032-9592\(03\)00207-3](https://doi.org/10.1016/S0032-9592(03)00207-3)
 36. Overend RP, Chornet E, Gascoigne J (1987) Fractionation of lignocellulosics by steam-aqueous pretreatments. *Philos Trans R Soc London A Math Phys Eng Sci* 321:523–536. <https://doi.org/10.1098/rsta.1987.0029>
 37. Peleteiro S, Garrote G, Santos V, Parajó JC (2014) Conversion of hexoses and pentoses into furans in an ionic liquid. *Afinidad* 71:202–206
 38. Bikker P, Krimpen MM, Wikselaar P et al (2016) Biorefinery of the green seaweed *Ulva lactuca* to produce animal feed, chemicals and biofuels. *J Appl Phycol* 28:3511–3525. <https://doi.org/10.1007/s10811-016-0842-3>
 39. Almeida JRM, Modig T, Petersson A, Hähn-Hägerdal B, Lidén G, Gorwa-Grauslund MF (2007) Increased tolerance and conversion of inhibitors in lignocellulosic hydrolysates by *Saccharomyces cerevisiae*. *J Chem Technol Biotechnol* 82:340–349
 40. Tsubaki S, Oono K, Hiraoka M, Ueda T, Onda A, Yanagisawa K, Azuma JI (2014) Hydrolysis of green-tide forming *Ulva* spp. by microwave irradiation with polyoxometalate clusters. *Green Chem* 16:2227–2233. <https://doi.org/10.1039/C3GC42027B>
 41. El Harchi M, Fakihi Kachkach FZ, El Mtili N (2018) Optimization of thermal acid hydrolysis for bioethanol production from *Ulva rigida* with yeast *Pachysolen tannophilus*. *S Afr J Bot* 115:161–169. <https://doi.org/10.1016/J.SAJB.2018.01.021>
 42. Kim DH, Lee SB, Jeong GT (2014) Production of reducing sugar from *Enteromorpha intestinalis* by hydrothermal and enzymatic hydrolysis. *Bioresour Technol* 161:348–353. <https://doi.org/10.1016/j.biortech.2014.03.078>
 43. Álvarez I, Condón S, Raso J (2006) Microbial inactivation by pulsed electric fields. pp 97–129
 44. Cemazar M, Sersa G, Frey W, Miklavcic D, Teissié J (2018) Recommendations and requirements for reporting on applications of electric pulse delivery for electroporation of biological samples. *Bioelectrochemistry* 122:69–76. <https://doi.org/10.1016/j.bioelechem.2018.03.005>
 45. Binder JB, Raines RT (2010) Fermentable sugars by chemical hydrolysis of biomass. *Proc Natl Acad Sci* 107:4516–4521. <https://doi.org/10.1073/pnas.0912073107>
 46. Lü X, Saka S (2012) New insights on monosaccharides' isomerization, dehydration and fragmentation in hot-compressed water. *J Supercrit Fluids* 61:146–156. <https://doi.org/10.1016/j.supflu.2011.09.005>
 47. Zhang B, Von Keitz M, Valentas K (2008) Thermal effects on hydrothermal biomass liquefaction. *Appl Biochem Biotechnol* 147:143–150. <https://doi.org/10.1007/s12010-008-8131-5>
 48. Boie W (1953) Fuel technology calculations. *Energietechnik* 3
 49. Grummel ES, Davies I (1933) A new method of calculating the calorific value of a fuel from its ultimate analysis. *Fuel* 12:199–203

50. Xu Q, Qian Q, Quek A, Ai N, Zeng G, Wang J (2013) Hydrothermal carbonization of macroalgae and the effects of experimental parameters on the properties of hydrochars. *ACS Sustain Chem Eng* 1:1092–1101. <https://doi.org/10.1021/sc400118f>
51. Haykiri-Acma H, Yaman S, Kucukbayrak S (2013) Production of briquettes from carbonized brown seaweed. *Fuel Process Technol* 106:33–40. <https://doi.org/10.1016/j.fuproc.2012.06.014>
52. Sun Y, Zhang JP, Wen C, Zhang L (2016) An enhanced approach for biochar preparation using fluidized bed and its application for H₂S removal. *Chem Eng Process Process Intensif* 104:1–12. <https://doi.org/10.1016/j.cep.2016.02.006>
53. Coates J (2006) Interpretation of infrared spectra, a practical approach. In: *Encyclopedia of analytical chemistry*
54. Pourhosseini SEM, Norouzi O, Naderi HR (2017) Study of micro/macro ordered porous carbon with olive-shaped structure derived from *Cladophora glomerata* macroalgae as efficient working electrodes of supercapacitors. *Biomass and Bioenergy* 107:287–298. <https://doi.org/10.1016/j.biombioe.2017.10.025>
55. Taskin E, de Castro BC, Allegretta I et al (2019) Multianalytical characterization of biochar and hydrochar produced from waste biomasses for environmental and agricultural applications. *Chemosphere* 233:422–430. <https://doi.org/10.1016/j.chemosphere.2019.05.204>

Publisher's Note Springer Nature remains neutral with regard to jurisdictional claims in published maps and institutional affiliations.